

# Development of beam emission spectroscopy in the helically symmetric experiment stellarator

Cite as: Rev. Sci. Instrum. **92**, 063503 (2021); <https://doi.org/10.1063/5.0043596>

Submitted: 09 January 2021 • Accepted: 11 May 2021 • Published Online: 01 June 2021

 S. Kobayashi, S. T. A. Kumar, F. S. B. Anderson, et al.

## COLLECTIONS

Paper published as part of the special topic on [Proceedings of the 23rd Topical Conference on High-Temperature Plasma Diagnostics](#)



View Online



Export Citation



CrossMark

## ARTICLES YOU MAY BE INTERESTED IN

[Development of a fast response neutron detector for the supersonic FRC collision process](#)  
Review of Scientific Instruments **92**, 063501 (2021); <https://doi.org/10.1063/5.0043609>

[Characterizing x-ray transmission through filters used in high energy density physics diagnostics](#)

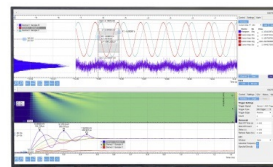
Review of Scientific Instruments **92**, 063502 (2021); <https://doi.org/10.1063/5.0043770>

[Ray-tracing analysis for cross-polarization scattering diagnostic on MAST-upgrade spherical tokamak](#)

Review of Scientific Instruments **92**, 063505 (2021); <https://doi.org/10.1063/5.0043600>

Challenge us.

What are your needs for  
periodic signal detection?



Zurich  
Instruments

# Development of beam emission spectroscopy in the helically symmetric experiment stellarator

Cite as: Rev. Sci. Instrum. 92, 063503 (2021); doi: 10.1063/5.0043596

Submitted: 9 January 2021 • Accepted: 11 May 2021 •

Published Online: 1 June 2021





View Online



Export Citation



CrossMark

S. Kobayashi,<sup>1,a)</sup>  S. T. A. Kumar,<sup>2</sup> F. S. B. Anderson,<sup>2</sup> C. B. Deng,<sup>2,3</sup> K. M. Likin,<sup>2</sup> J. N. Talmadge,<sup>2</sup> S. Ohshima,<sup>1</sup>  and D. T. Anderson<sup>2</sup>

## AFFILIATIONS

<sup>1</sup>Institute of Advanced Energy, Kyoto University, Uji, Kyoto 611-0011, Japan

<sup>2</sup>Department of Electrical and Computer Engineering, University of Wisconsin-Madison, Madison, Wisconsin 53706, USA

<sup>3</sup>Department of Physics, University of California, Los Angeles, Los Angeles, California 90095, USA

**Note:** Paper published as part of the Special Topic on Proceedings of the 23rd Topical Conference on High-Temperature Plasma Diagnostics.

<sup>a)</sup>Author to whom correspondence should be addressed: [kobayashi@iae.kyoto-u.ac.jp](mailto:kobayashi@iae.kyoto-u.ac.jp)

## ABSTRACT

This study shows the feasibility of a beam emission spectroscopy (BES) diagnostic in the Helically Symmetric eXperiment (HSX) stellarator for obtaining the spatiotemporal structure of density fluctuation. A beam emission simulation was applied to HSX plasmas to design and optimize viewing chords and to estimate the beam emission spectrum. A Doppler-shifted beam emission spectrum was measured from a 30 kV, 4 A diagnostic neutral beam injected into HSX plasmas. The beam emission was measured with a high-time-resolution avalanche photodiode (APD) assembly to determine the feasibility of BES in HSX. For HSX plasmas heated by 28 GHz electron cyclotron heating, a mode around  $f = 15$  kHz was observed in the BES signal. The coherence between the BES signal and the density fluctuation measured by an interferometer system was significant. A plan for improving the BES system to enable the measurement of higher frequency related to turbulent transport is presented. The array of sightlines proposed in this study can be used to measure beam emission with a Doppler shift larger than 3 nm (blue shift), which enables the use of a wide passband interference filter to obtain higher throughput. The adoption of a large objective optics and a chilled APD assembly will improve the signal-to-noise ratio.

Published under license by AIP Publishing. <https://doi.org/10.1063/5.0043596>

## I. INTRODUCTION

The study of magnetohydrodynamic (MHD) and turbulent transport has long been an important subject not only for understanding anomalous transport but also for clarifying physical mechanisms of transitions to improved confinement modes such as H-mode in magnetically confined fusion plasmas. The technique of beam emission spectroscopy (BES) has been developed for the study of MHD and turbulent transport in many torus devices.<sup>1-5</sup> The spatiotemporal structure of density fluctuations has been evaluated using spectral measurements of Doppler-shifted  $H_\alpha/D_\alpha$  light emissions followed by the collisional excitation process between the hydrogen or deuterium neutral beam atoms and plasmas. This kind of active beam spectroscopy can be used to obtain localized and long-wavelength fluctuations ( $k\rho_i < 1$ ).

The Helically Symmetric eXperiment (HSX) stellarator is a medium-sized stellarator device ( $R/a = 1.2/0.15$  m) that has quasi-helically symmetric magnetic configurations formed by modular coils.<sup>6</sup> The turbulent transport studies in HSX have been carried out by utilizing a multichannel interferometer diagnostic using the far-forward scattering technique.<sup>7</sup> However, localized density fluctuation measurements are of interest to clarify the spatial structure of the turbulence and its relation to the transport. In HSX, a 30 kV, 4 A hydrogen diagnostic neutral beam (DNB) has been applied for active beam spectroscopy.<sup>8,9</sup> To apply active beam spectroscopy to three-dimensional magnetic configurations, it is important to estimate the observation position and the spatial resolution, which depend on the spatial distribution of the beam density, flux surface structure, and sightline path. Moreover, beam smearing due to the finite lifetime of the excited state of the beam atoms affects the estimation. In this study, we apply the beam emission simulation developed in

our previous study<sup>5</sup> to design suitable sightlines for BES in HSX. The feasibility of density fluctuation measurements is discussed for a high-time-resolution avalanche photodiode (APD) assembly.

## II. BEAM EMISSION SIMULATION

### A. Simulation scheme

In this section, we describe the beam emission simulation for HSX to calculate the observation position and the Doppler shift of the beam emission for the design of viewing chords. The simulation code calculates the beam emission intensity  $I_{BE}$  along a sightline  $l$ , which is determined by the following formula:<sup>5</sup>

$$I_{BE} = \int dl \frac{A_{32}}{A_{32} + A_{31}} (n_i n_{beam} \sigma_i v_{beam} + n_e n_{beam} \times \langle \sigma_e | v_{beam} - v_e | \rangle) \times h\nu S \Delta\Omega/4\pi, \quad (1)$$

where  $A_{nm}$  is the transition probability from the  $n$  to  $m$  states;  $n_i$ ,  $n_e$ , and  $n_{beam}$  are the ion, electron, and neutral beam densities, respectively; and  $v_e$  and  $v_{beam}$  are the electron thermal and beam velocities, respectively. The effect of thermal velocity on bulk ions is negligible because the ion temperature [ $T_i(0) \sim 60$  eV] is below the injected DNB energy. For an electron temperature  $T_e$  of around 1 keV, the effective cross section of the electron impact excitation ( $\langle \sigma_e | v_{beam} - v_e | \rangle / v_{beam} \sim 1.7 \times 10^{-17}$  cm<sup>2</sup>) is almost the same as that for an ion ( $\sigma_i$ ). This means that the separation of ion and electron density fluctuations in the beam emission signal of HSX is difficult.  $S$  and  $\Delta\Omega/4\pi$  are the observation area along the sightline element  $dl$  and the solid angle, respectively.

The beam emission was simulated using the following scheme: (1) determine the spatial profile of the beam density with the beam attenuation effect, (2) calculate the beam emission distribution with the beam smearing effect taken into account, and (3) estimate the spatial resolution and spectral profile of the beam emission from a selected viewing chord. To determine the spatial profile of the beam emission, an inverse mapping from the real coordinate system ( $r, z, \phi$ ) to the magnetic (Boozer) coordinate system ( $s, \theta, \zeta$ ) is used. Because the cross section at a toroidal angle  $\zeta$  in the Boozer coordinate system is curved significantly in the real coordinate system, the inverse mapping uses a full-width search method. In this simulation, the beam size was set to  $\phi = 30$  mm. The lifetime of the excited state of the beam atoms affects the spatial resolution and observation position of the beam emission line. Therefore, the beam smearing effect was taken into account in the simulation. From the lifetime of the excited state, the beam atoms from the DNB can travel around 5 cm after electron/ion impact excitations; however, the smearing distance is reduced to about 1/3 when the multistep transition model is considered.<sup>1</sup> In this study, the effective smearing distance for the  $H_\alpha$  line was set to 1 cm as an input to the simulation.

### B. Estimation of beam emission profile and comparison to spectrum measurement

The Doppler shift of the beam emission was calculated using two arrays of sightlines. Figure 1 shows a schematic view of the sightlines considered for a beam emission diagnostic for the HSX device. One array of sightlines (array A in the figure) has ten sightlines and is set from a viewing port that observes redshifted beam emission spectra. The spectral profile of the beam emission

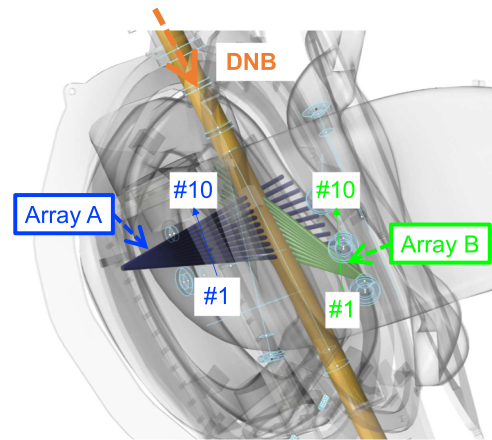


FIG. 1. Schematic view of the array of sightlines for the BES diagnostic in HSX. Each array has ten sightlines that observes the diagnostic neutral beam at positions from  $r/a = 0.1$  to  $0.9$ .

line and observation position calculated by the simulation code is plotted in Fig. 2(a) by the dotted lines. The beam energy distribution was assumed to be monochromatic ( $E_b = 30$  keV) in this calculation. The Doppler shift of the beam emission from this port

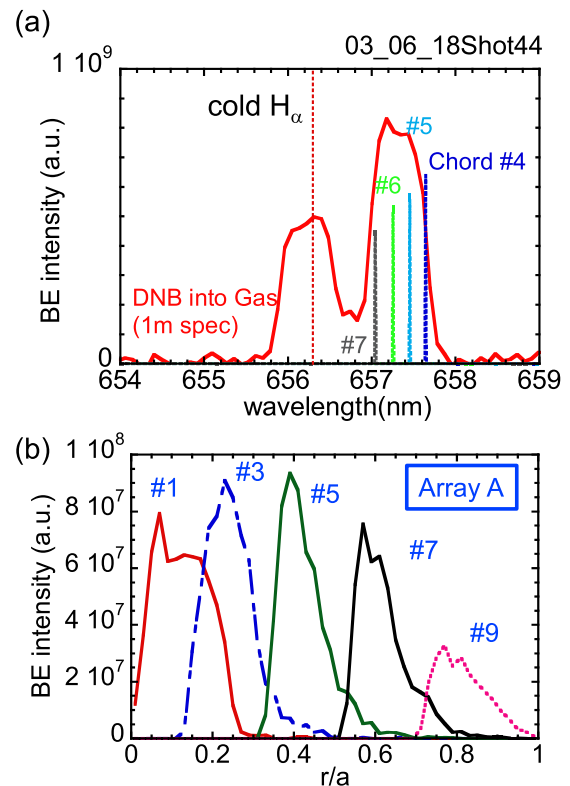


FIG. 2. (a) Comparison of the beam emission spectrum measured using a monochromator with simulated beam emission and (b) spatial profile of beam emission intensity along various sightlines of array A.

was calculated to be about 1 nm. The observation position and spatial resolution of a sightline were calculated by summing up the locations of the beam emission along a sightline. Figure 2(b) shows the beam emission intensity profile as a function of the normalized minor radius  $r/a$ . Due to the smearing effect, each chord has an asymmetric profile with an extended tail in the outside direction. The center-of-gravity and the dispersion of the profile provide information on the measurement location and resolution of a sightline, respectively. The simulation results show that the array of sightlines has a measurement location from  $r/a = 0.1$  to  $0.9$  with a spatial resolution of  $\Delta r/a = \pm 0.07$ . In this case, each interval between adjacent sightlines  $\Delta r$  is about 2 cm, which corresponds to an effective interval normalized by the minor radius  $\Delta r/a$  of 0.1. This resolution yields the Nyquist wavenumber in the radial direction,  $k_r = \pi/\Delta r$ , less than 1.6 rad/cm, that is,  $k_r \rho_i < 0.3$  by assuming the typical ion temperature observed in the HSX plasmas. Although the measurable wavenumber for the sightlines is limited to obtain density fluctuations by turbulence, the feasibility study can be carried out by measuring density fluctuations induced by MHD activities.

To confirm the simulation results, the Doppler shift of the beam spectrum was measured when the DNB was injected into the HSX device filled with hydrogen gas. In this case, the beam emission caused by collisions with the hydrogen gas was observed with a monochromator ( $f = 1$  m) with a chilled CCD camera. We used an objective optical system that has been used for the motional stark effect diagnostic in HSX.<sup>9</sup> The obtained spectrum, plotted in Fig. 2(a) by the solid line, indicates that the simulated beam emission spectra are consistent with the measurement results when the observation position is around  $r/a = 0.4$ – $0.5$ .

### III. DENSITY FLUCTUATION MEASUREMENT WITH AVALANCHE PHOTODIODE ASSEMBLY

To determine the feasibility of density fluctuation measurement with BES, an APD assembly was applied to the interference filter and full width at half maximum of 0.5 nm. The APD assembly (Scientex, M-100) used in this study has a frequency range from DC to 200 kHz and a maximum quantum efficiency of 85% at  $\lambda = 650$  nm. Its sensitivity is  $2.8 \times 10^8$  V/W at  $\lambda = 800$  nm. Prior to the experiment, the center wavelength of the interference filter was tuned to 657.7 nm by controlling the filter temperature to reduce contamination of the beam emission signal by the cold  $H_\alpha$  component and to obtain the maximum throughput of the beam emission when the DNB was injected into the hydrogen gas. The sightline was the same as that used for the spectrum measurement described in Sec. II. Figure 3 shows the time evolution of the electron density measured by the interferometer and the beam emission signal obtained by the APD assembly. Plasma with an electron density of around  $4 \times 10^{18} \text{ m}^{-3}$  was formed by 28 GHz, 50 kW electron cyclotron heating (ECH). A significant beam emission signal was observed when the DNB was turned on. Because the APD signal is quite small before and after DNB injection, the contamination of the beam emission signal by the cold  $H_\alpha$  component or impurity lines is thought to be negligible. This means that the beam emission line can be separated by the interference filter, while the Doppler shift of the beam emission line from the cold  $H_\alpha$  component is around 1 nm.

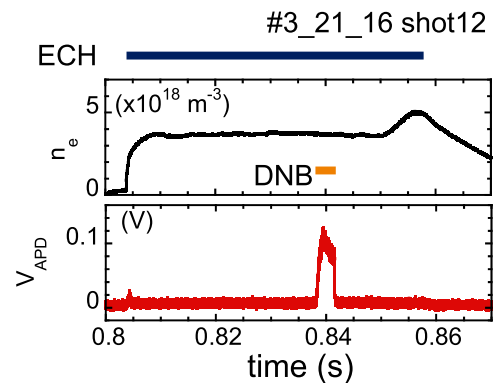


FIG. 3. Time evolution of the line-averaged electron density and BES signal observed for 28 GHz ECH plasmas of HSX.

The power spectra of the density fluctuations measured by the interferometer (central chord) and APD ( $r/a = 0.4$ ) are shown in Figs. 4(a) and 4(b), respectively. The beam emission spectrum with the APD assembly averaged over the period during DNB injection ( $t = 0.8385$ – $0.8408$  s) is plotted by a bold solid line. At the frequency above 5 kHz, the noise level of the APD signal obtained during the DNB turn-off phase [dotted line in Fig. 4(b)] is almost the same level

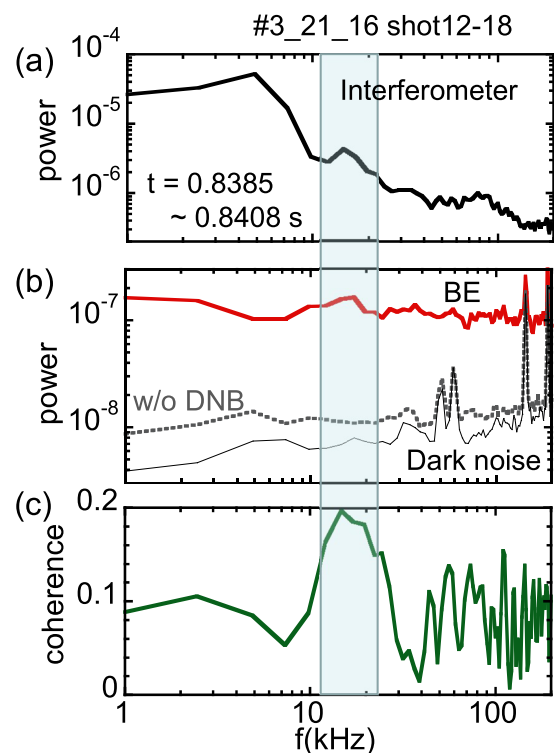


FIG. 4. Power spectrum of (a) the density fluctuation measured by the interferometer and (b) APD signals and (c) the coherence between interferometer and beam emission signals.

as that for the dark noise (narrow solid line). The power spectrum of the interferometer signal shows an existence of a coherent mode around  $f = 15$  kHz, which has been observed in the ECH plasma of HSX as a core-localized mode.<sup>10</sup> A relatively small response in the power spectrum of the beam emission can be seen in the frequency range of the core-localized mode. A relatively low coherence ( $\sim 0.2$ ) between the interferometer and BES signals shown in Fig. 4(c) is attributed to that the core-localized mode had an odd poloidal mode number,<sup>11</sup> and we have not applied the inversion technique to the interferometer signal. Despite the inconsistency of the measurement locations between the two density fluctuations, the coherence indicates that the developed BES system can obtain the density fluctuations in the ECH plasma of HSX. However, the signal level is not high enough to measure the density fluctuation at frequencies higher than 50 kHz. A modification to the BES system to enable measurements at higher frequencies is presented in Sec. IV.

#### IV. DISCUSSIONS AND SUMMARY

To observe high frequency ( $>50$  kHz) density fluctuations regarding turbulent transport, the signal-to-noise ratio of the system must be increased. The observed intensity level indicates  $3 \times 10^4$  photons per time response for the APD ( $5 \mu\text{s}$ ), which corresponds to a shot-noise (photon-noise) level of 0.6% of the observed intensity if the photon emission obeys the Poisson distribution. To increase the signal intensity and to reduce the noise level to below 0.2%, we propose the following modified design for the BES system.

An array of sightlines that is closer to the beam can be adopted. As shown in Fig. 1, array B observes the blueshifted beam emission

with a shallow angle to the beam line. The beam emission simulation expects that the beam emission intensity, shown in Fig. 5(a), is around 4–5 times higher than that from array A (see Sec. II). This is due to the distance between the viewing port and the beam being reduced by about half. The benefit of applying the closer array of sightlines in BES is that a relatively large Doppler-shift (in the range of 2.8–4.2 nm) is obtained, which allows the use of an interference filter with a wider bandwidth and higher transmittance. As shown in Fig. 5(b), the sightlines of array B can observe the radial profile of the density fluctuations from  $r/a = 0.1$  to 0.9 with a radial resolution of  $\Delta r/a = \pm 0.06$  to  $\pm 0.08$ . Although the Nyquist wavenumber  $k_r$  of the sightlines is almost the same as that for the sightlines of array A, an improvement in the ion temperature up to several hundreds of eV using a high power 70 GHz ECH planned in HSX will enable the detection of ion scale turbulence. Chilling the APD assembly to below  $-20^\circ\text{C}$  reduces the electrical noise by 30%.<sup>12</sup> In addition to the above design, an objective optical system with a low F number will reduce the noise level of the BES system to below 0.2%.

In summary, we carried out the beam emission simulation to design the BES system for HSX. The feasibility study using the APD assembly showed that the noise level in the beam emission line was 0.6% of the intensity. The array of sightlines proposed in this study allows the use of the high throughput interference filter. The improvements to the BES system described here will further reduce the noise level of the system.

#### ACKNOWLEDGMENTS

The authors would like to thank the member of the HSX group for conducting the experiments. This work was supported by the JSPS Grants-in-Aid for Scientific Research (No. 19H01875); “PLADyS” JSPS Core-to-Core Program, A. Advanced Research Networks; Japan/U.S. Cooperation in Fusion Research and Development; and the Future Energy Research Association.

#### DATA AVAILABILITY

The data that support the findings of this study are available from the corresponding author upon reasonable request.

#### REFERENCES

- R. J. Fonck, P. A. Duperrex, and S. F. Paul, *Rev. Sci. Instrum.* **61**, 3487 (1990).
- R. D. Durst, R. J. Fonck, G. Cosby, H. Evensen, and S. F. Paul, *Rev. Sci. Instrum.* **63**, 4907 (1992).
- G. McKee, R. Ashley, R. Durst, R. Fonck, M. Jakubowski, K. Tritz, K. Burrell, C. Greenfield, and J. Robinson, *Rev. Sci. Instrum.* **70**, 913 (1999).
- T. Oishi, S. Kado, M. Yoshinuma, K. Ida, S. Tanaka, and S. Okamura, *J. Plasma Fusion Res.* **6**, 449 (2004).
- S. Kobayashi, S. Kado, T. Oishi, S. Ohshima, T. Kagawa, Y. Nagae, S. Yamamoto, T. Mizuuchi, K. Nagasaki, H. Okada *et al.*, *Rev. Sci. Instrum.* **83**, 10D535 (2012).
- A. F. Almagri, D. T. Anderson, F. S. B. Anderson, P. H. Probert, J. L. Shohet, and J. N. Talmadge, *IEEE Trans. Plasma Sci.* **27**, 114 (1999).
- C. B. Deng, D. L. Brower, D. T. Anderson, F. S. B. Anderson, A. Briesemeister, and K. M. Likin, *Nucl. Fusion* **55**, 123003 (2015).
- G. F. Abdrashitov, V. I. Davydenko, P. P. Deichuli, D. J. Den Hartog, and G. Fiksel, *Rev. Sci. Instrum.* **72**, 594 (2001).

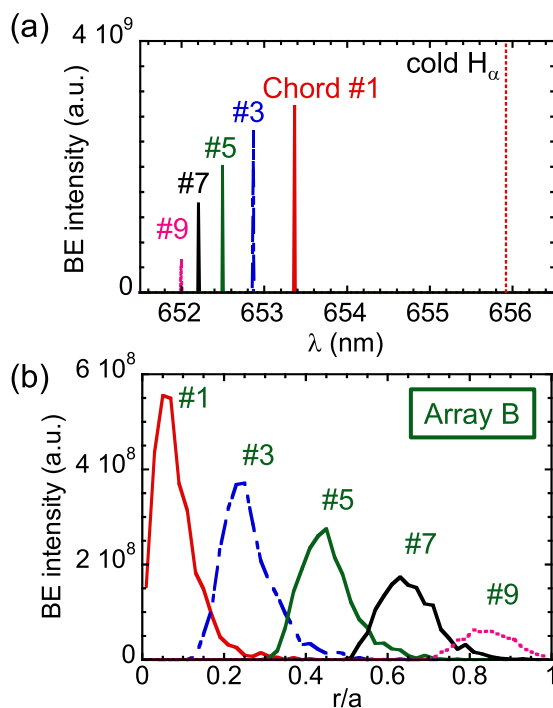


FIG. 5. (a) Spectral and (b) spatial profiles of the beam emission line from array B.

<sup>9</sup>T. J. Dobbins, S. T. A. Kumar, and D. T. Anderson, *Rev. Sci. Instrum.* **87**, 11D413 (2016).

<sup>10</sup>C. B. Deng and D. L. Brower, *Rev. Sci. Instrum.* **83**, 10E308 (2012).

<sup>11</sup>C. B. Deng, D. L. Brower, D. T. Anderson, F. S. B. Anderson, A. Briesemeister, K. Likin, J. Lore, J. Schmitt, J. N. Talmadge, R. Wilcox, and K. Zhai, “Core density

fluctuation measurements by interferometry in the HSX stellarator,” in APS-DPP Meeting, Salt Lake City, 2011.

<sup>12</sup>S. Kobayashi, S. Ohshima, H. Matsuda, X. X. Lu, D. Kokubu, K. Ida, T. Kobayashi, M. Yoshinuma, S. Kado, T. Oishi *et al.*, *Rev. Sci. Instrum.* **87**, 11E519 (2016).